ELSEVIER

Surface Science 345 (1996) L1–L10

surface science

Surface Science Letters

Multilayer adsorption and desorption: Au and Cu on Mo(110)

S.H. Payne [a], H.J. Kreuzer [a,*], A. Pavlovska [b], E. Bauer [b]

[a] *Department of Physics, Dalhousie University, Halifax, NS, Canada B3H 3J5*
[b] *Physikalisches Institut, Technische Universität Clausthal, D-3392 Clausthal-Zellerfeld, Germany*

Received 18 August 1995; accepted for publication 19 September 1995

Abstract

We use a multilayer lattice gas model for adsorption and desorption to analyze data on Cu/Mo(110) and Au/Mo(110) extracting surface binding energies and lateral interactions. We establish layer-by-layer growth for the first two layers.

Keywords: Copper; Gold; Ising models; Low index single crystal surfaces; Models of surface kinetics; Molybdenum; Thermal desorption; Thermal desorption spectroscopy

Whereas adsorbates with mainly repulsive lateral interactions are generally restricted to the submonolayer regime, those with mainly attractive lateral interactions exhibit multilayer growth. Examples of the latter are most physisorbed systems such as rare gases and inert molecules on metals or insulators, but also strongly chemisorbed systems such as noble metals on transition metals and others [1]. Although such systems have been studied experimentally for many years and are obviously of great interest and importance, little progress has been made on the theoretical side despite major advances in our understanding of adsorption and desorption in monolayer adsorbates. Recently, Payne and Kreuzer have presented a theory of multilayer adsorption and desorption based on a lattice gas [2]. In this paper we will use this theory to fit and analyze experimental data on Cu on Mo(110) [3] and Au on Mo(110) [4].

Our main interest is in the adsorption and desorption kinetics of the first two layers where effects of the adsorbate–substrate interaction are still at play. Our model is based on a lattice gas with a Hamiltonian [2]

$$H = E_{s1}\sum_i n_i + E_{s2}\sum_i n_i m_i + \tfrac{1}{2}V_{11}\sum_{\text{n.n.}} n_i n_j + \tfrac{1}{2}V'_{11}\sum_{\text{n.n.n.}} n_i n_j + V_{12}\sum_{\text{n.n.}} n_i m_i n_j + \tfrac{1}{2}V_{22}\sum_{\text{n.n.}} n_i m_i n_j m_j + \tfrac{1}{2}V'_{22}\sum_{\text{n.n.n.}} n_i m_i n_j m_j + \ldots . \quad (1)$$

Here the occupation number $n_i = 0$ or 1 depending on whether site i is empty or has a particle adsorbed in the first layer with a single particle energy E_{s1}. Likewise, $m_i = 0$ or 1 depending on whether the site i in the second layer is empty or occupied with an energy E_{s2}. In this report we assume on-top sites for the second layer as this is by far the simpler calculation, and we do not expect drastic changes as one goes to multi-coordinated higher layer sites. In Eq. (1) we identify V_{11} (V'_{11}) and V_{22} (V'_{22}) as the lateral

* Corresponding author. Fax: +1 902 4945191; E-mail: phys@ac.dal.ca.

SSDI 0039-6028(95)00969-8

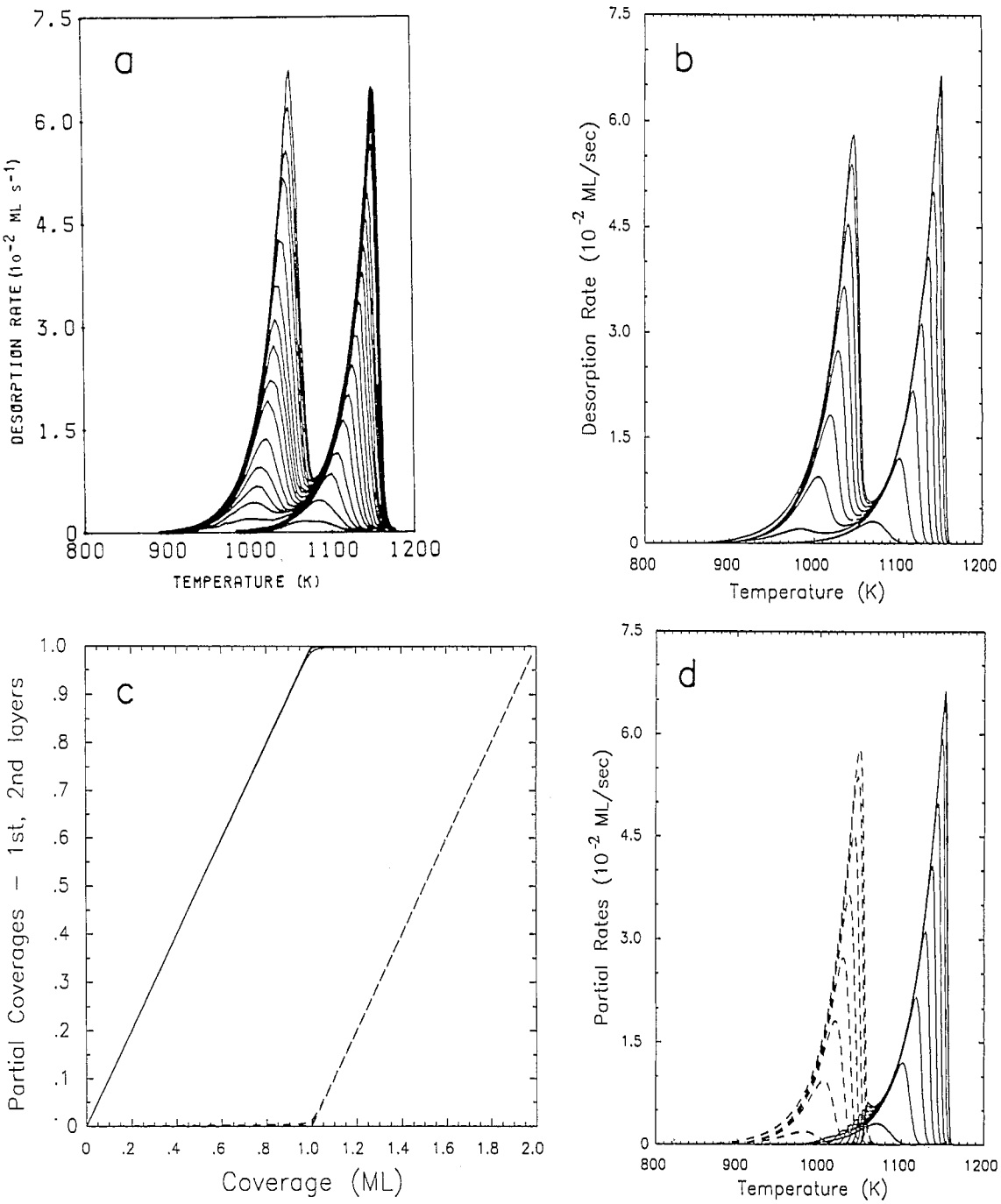

Fig. 1. (a) TPD data of the first two monolayers of Cu on Mo(110) obtained with a heating rate of 2.43 K s^{-1}. The curves differ in initial coverage by approximately 0.07 monolayers between 0.07 and 2.2 monolayers. (b) Theoretical fit for initial coverages between 0.07 and 2 monolayers in steps of 0.14 with the following parameters: $V_0^{(1)} = 3.2$ eV, $V_0^{(2)} = 2.98$ eV, $V_{11} = -0.172$ eV, $V_{12} = 0$ eV, $V_{22} = -0.129$ eV, $\nu_x = \nu_y = \nu_z = 5 \times 10^{12}$ s^{-1}. (c) Partial coverages for first (———) and second (- - -) layers as a function of temperature. (d) Partial rates for first (———) and second (- - -) layers as a function of temperature. (e) Isosteric heat of adsorption for $T = 900$, 1000, 1100, 1200 K (top to bottom at low θ). Dashed line is the desorption energy obtained from an isosteric Arrhenius analysis of the theoretical curves. (f) Effective prefactor from the Arrhenius analysis of the theoretical curves. (g), (h) The corresponding experimental data.

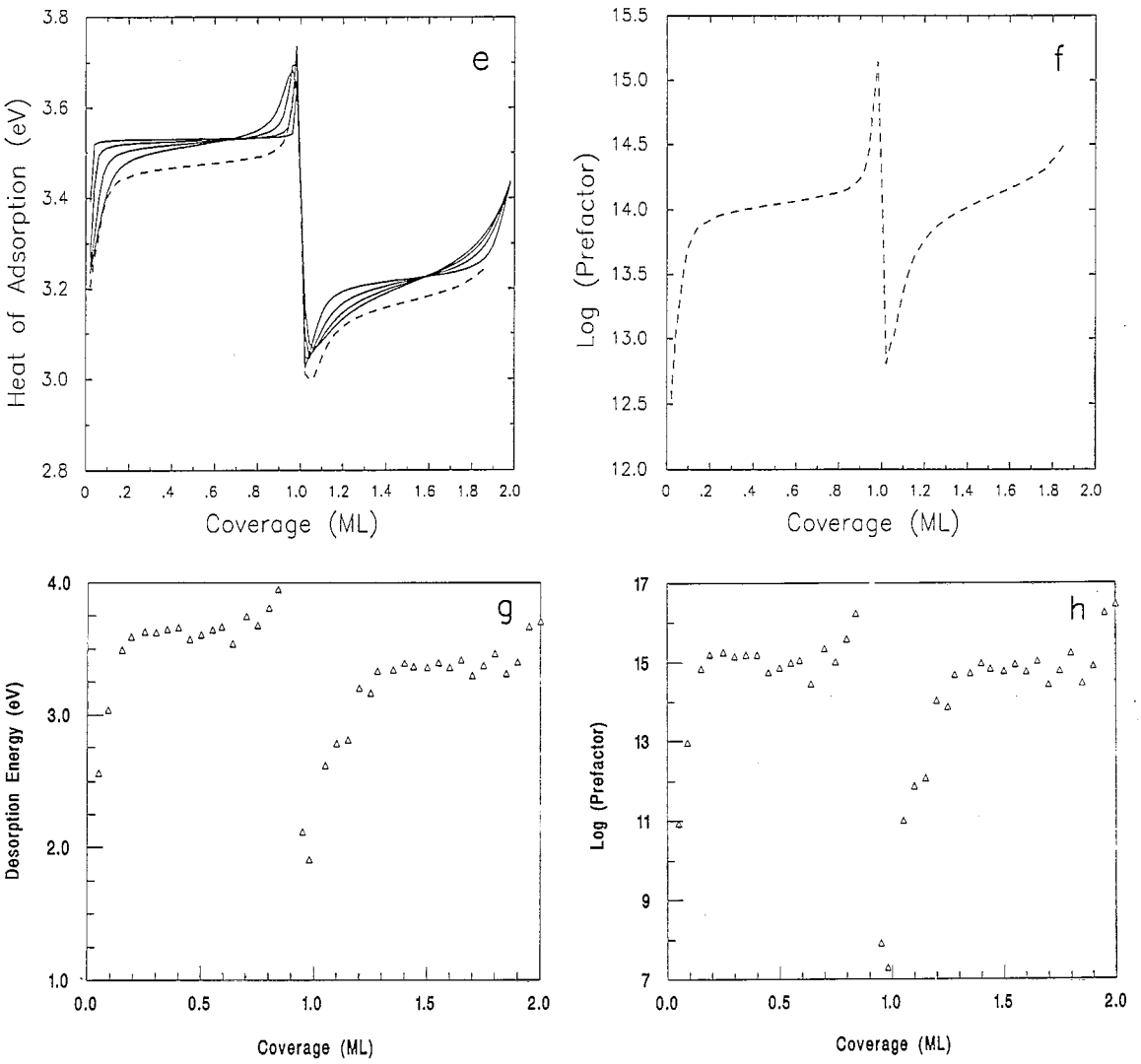

Fig. 1 (continued).

interactions between two particles in nearest neighbor (next-nearest neighbor) sites in the first and second layers, respectively. The interaction V_{12} is between next-nearest neighbors with one particle in the first layer and the second in the second layer. The nearest neighbor interaction between a particle in the first layer and another one on top of it in the second layer is accounted for by E_{s2}, which also contains the residual interaction with the substrate.

As long as the number of particles in the adsorbate does not change, which is the case for systems in equilibrium, or for diffusion studies, the single particle terms in Eq. (1) are constant and can be dropped from further consideration. However, if we want to study adsorption–desorption kinetics, the number of particles in the adsorbate changes as a function of time and a proper identification of E_s is mandatory. Arguing that the lattice gas Hamiltonian should give the same Helmholtz free energy as a microscopic Hamiltonian (for non-interacting particles), one can show that the proper identification is given by [5]

$$E_{s1} = -V_0^{(1)} - k_B T \ln\left(q_3^{(1)}\right) \tag{2}$$

and a similar expression for E_{s2}. Here $V_0^{(1)}$ is the (positive) binding energy of an isolated adparticle in the first layer. $V_0^{(2)}$ is the binding energy of a single adparticle in the second layer atop an isolated particle in the first layer, i.e. the difference $V_0^{(2)} - V_0^{(1)}$ accounts for the interaction between these particles and the shielding action of the first layer on the interaction of the second layer with the substrate. q_3 is a partition function for the vibrations of the adparticle with respect to the substrate, which we approximate by three harmonic oscillators accounting for the motion perpendicular and parallel to the surface.

To model the adsorption–desorption kinetics we will assume that fast surface diffusion (fast on the time scale of adsorption and desorption) maintains the adsorbate in quasi-equilibrium. In such situations the system is completely characterized by the coverage, θ, and we get the adsorption and desorption rates to be [2,6]

$$R_{ad} = S(\theta,T)\, a_s \frac{\lambda}{h} P, \tag{3}$$

$$R_{des} = S(\theta,T)\, a_s \frac{k_B T}{h\lambda^2 q_3} \times \exp\left[\left(-V_0^{(1)} + \mu_{ad}(\theta,T)\right)/k_B T\right], \tag{4}$$

with a_s the area of an adsorption site, $\lambda = (2\pi m k_B T)^{1/2}$ the thermal wavelength of a particle of mass m, $S(\theta,T)$ is the sticking coefficient, and P the instantaneous pressure. The dependence of the desorption rate on the binding difference $\Delta V_0 = V_0^{(1)} - V_0^{(2)}$ and the lateral interaction energies such as V_{11}, V_{22}, etc., is accounted for in the chemical potential, $\mu_{ad}(\theta,T)$.

To complete the theory we need (i) to specify the coverage dependence of the sticking coefficient and (ii) to calculate the chemical potential of the adsorbate from the Hamiltonian (1). The sticking coefficient is a measure for the efficiency of energy transfer in adsorption and desorption. As such it cannot be obtained from thermodynamic arguments but must be calculated from a microscopic theory or can be postulated in a phenomenological approach, based on experimental evidence for a particular system or some simple arguments. For interacting systems it is generally both coverage and temperature dependent; however, for metals on metals the sticking coefficient is observed to be independent of coverage, and we will assume this below.

We obtain the chemical potential by employing the transfer matrix method [2]. The transfer matrix is constructed for interactions between particles in pairs of adjacent rows of M adsorption sites in the finite direction. Its leading eigenvalue, λ_1, gives the grand partition function, $\Xi(T,M,\mu) \approx \lambda_1^M$, and hence the coverage

$$\theta = \frac{k_B T}{M} \left.\frac{\partial \ln \Xi}{\partial \mu}\right|_T. \tag{5}$$

The partial coverages of the first and second layers are obtained from $\theta_1 = \Sigma_i \langle n_i \rangle$ and $\theta_2 = \Sigma_i \langle m_i \rangle$. Exact results can be obtained by this method for large enough M. In practice, it suffices to consider only the totally symmetric subblock of the transfer matrix for this calculation; θ is obtained from the corresponding eigenvector. We have performed all our calculations for $M = 6$ on a centered rectangular lattice.

We now turn to our first system, Cu on Mo(110) [3]. Experimental TPD (temperature programmed desorption) traces are reproduced in Fig. 1a with a theoretical fit given in Fig. 1b. Although we have assumed isotropic nearest neighbor interactions alone with on-top adsorption for the second layer, the model reproduces the experimental data surprisingly well, with regard to both the shape of the desorption traces as well as the absolute magnitude of the rates. The binding energy of an isolated Cu atom in the first layer, $V_0^{(1)}$, and its vibrational frequencies, ν_x, ν_y, ν_z (assumed equal for simplicity) are obtained by simultaneously fitting the peak position of the lowest coverage TPD trace, where interactions are negligible, and the temperature dependence of the isothermal desorption rates [3]. We find $V_0^{(1)} = 3.2$ eV and $\nu_x = \nu_y = \nu_z = 5 \times 10^{12}$ s^{-1}, in perfect agreement with earlier estimates based on simple monolayer models. A single atom in the second layer is bound marginally weaker with $V_0^{(2)} = 2.98$ eV. We recall that this energy is composed of the residual interaction with the Mo substrate and of the nearest neighbor interaction with the underlying Cu atom. Lateral nearest neighbor interactions in the first and second layers are attractive, we have set $V_{11} = -0.172$ eV and $V_{22} = -0.129$ eV. This gives a critical tempera-

ture of the first layer of $T_c = 1125$ K in agreement with an estimate by Paunov and Bauer from TPD data [3]. It is not surprising that V_{11} is larger than the earlier estimates [3] based on Bragg–Williams and improved quasichemical approximations as the latter consistently underestimate the critical temperature for a given V_{11}, and thus overestimate V_{11} in a fit of the experimental T_c. Desorption from the coexistence region of the first layer is quite clearly displayed in the leading edge of the high temperature TPD peaks indicative of zero-order desorption. The evidence for coexistence in the second layer is not as straightforward because of the early break of the TPD traces from the leading edge for coverages between 1 and about 1.5 monolayers. Even if for larger initial coverages desorption is out of a coexistence region this still suggests that the lateral attraction in the second layer is smaller than it is in the first as evidenced by our fit parameters. Indeed, if we make $V_{22} = V_{11}$, the quality of the fit is worse with clear evidence for coexistence in the low temperature TPD peaks. It appears surprising that the nearest neighbor attraction in the second layer is less than in the first. One expects it to be larger in the second layer as a result of the weaker bonding to the surface. However, the double layer is considerably strained, which makes it easier to remove atoms from the second layer. The increasing strain with increasing thickness is also reflected in the termination of the layer-by-layer growth after completion of the double layer [1]. To the extent that V_{22} is uncertain so is ΔV_0, as the latter determines the separation of the two peaks.

The growth mode of the Cu bilayer is shown in Fig. 1c as the partial coverages θ_1 and θ_2 of the first and second layer, respectively, as a function of total coverage for temperatures spanning the desorption range. Layer-by-layer growth is clearly in evidence with negligible mass transfer to the second layer below a monolayer even at the highest temperatures. Layer-by-layer growth has an interesting effect on the partial rates $d\theta_1/dt$ and $d\theta_2/dt$, Fig. 1d, in the intermediate temperature range of TPD where first and second layer peaks overlap: although the partial rates show apparent independent desorption of the two layers with the first layer trailing the second at higher temperatures, desorption from the first layer is now constrained by that of the second layer, resulting in a sudden onset of the former and a shift of the first layer peak for initial coverages larger than one monolayer to higher temperatures to accommodate the total amount of material to be desorbed.

In Fig. 1e we show the isosteric heat of adsorption

$$Q_{\mathrm{iso}}(\theta,T) = k_{\mathrm{B}}T^2 \left.\frac{\partial \ln P}{\partial T}\right|_{\theta} \tag{6}$$

for various temperatures where P is the equilibrium pressure to maintain a coverage θ at temperature T. It consists essentially of the isosteric heats of two independent layers. Starting at zero coverage and low temperature the sharp rise in Q_{iso} signifies increasing clustering in a two-dimensional gas. Once the phase boundary is reached Q_{iso} becomes independent of coverage, indicative of coexistence, but rising again towards the completion of the first monolayer to establish the last available bonds. The sharp drop at a monolayer reflects the fact that isolated second layer particles are bound less tightly to the underlying first layer and the substrate than their kin are in the first layer, i.e. $Q_{\mathrm{iso}}(\theta = 0,T) - Q_{\mathrm{iso}}(\theta = 1+,T) = \Delta V_0$.

Also given in Fig. 1e is the desorption energy as obtained from an isosteric Arrhenius analysis [7] of the theoretical curves of Fig. 1b. We recall [6] that for a system that is kept in quasi-equilibrium during desorption by fast surface diffusion, the desorption energy is a temperature average of the isosteric heat of adsorption (displaced by $k_{\mathrm{B}}T/2$). In Fig. 1f we show the corresponding prefactor. When comparing the desorption energy obtained from the theoretical fit with that obtained by Paunov and Bauer by an isosteric analysis of their data [3] we noted a marked discrepancy, namely that just below a monolayer the theoretical desorption energy exhibits an upswing whereas the experimental data show a marked decrease starting around 0.8 of a monolayer to a much lower value at a monolayer. We have therefore analyzed newer experimental data [8] with the ASTEK programme [7] obtaining Figs. 1g and 1h for desorption energy and prefactor, respectively. The agreement between theoretical and experimental analyses is excellent including the upswings just below one and two monolayers. The rather low values just below a monolayer are undoubtedly artifacts arising from very poor isosteres as a result of

the fact that we had to digitize the experimental desorption traces from plotter output. Although there might be arguments why desorption energies should dip so low, prefactors below 10^{12} s^{-1} are hard to explain except as a result of sticking coefficients substantially lower than unity, which is not comprehensible for this system. One should therefore discard the lowest four points just above a monolayer in the desorption energy and the prefactor.

In our model of the Cu/Mo(110) system we have included nearest neighbor attractions in the two layers, V_{11} and V_{22}, but neither trio nor next-nearest neighbor interactions, V'_{11}, V'_{22} and V_{12}. Indeed, in layer-by-layer growth the effect of V_{12} can be subsumed into ΔV_0 by replacing it by $\Delta V_0 - V_{12}/4$ because a particle in the second layer always sees a completed layer under it so that the correlation function $\langle n_i n_{i+a} m_i \rangle = \langle m_i \rangle$. The effect of including

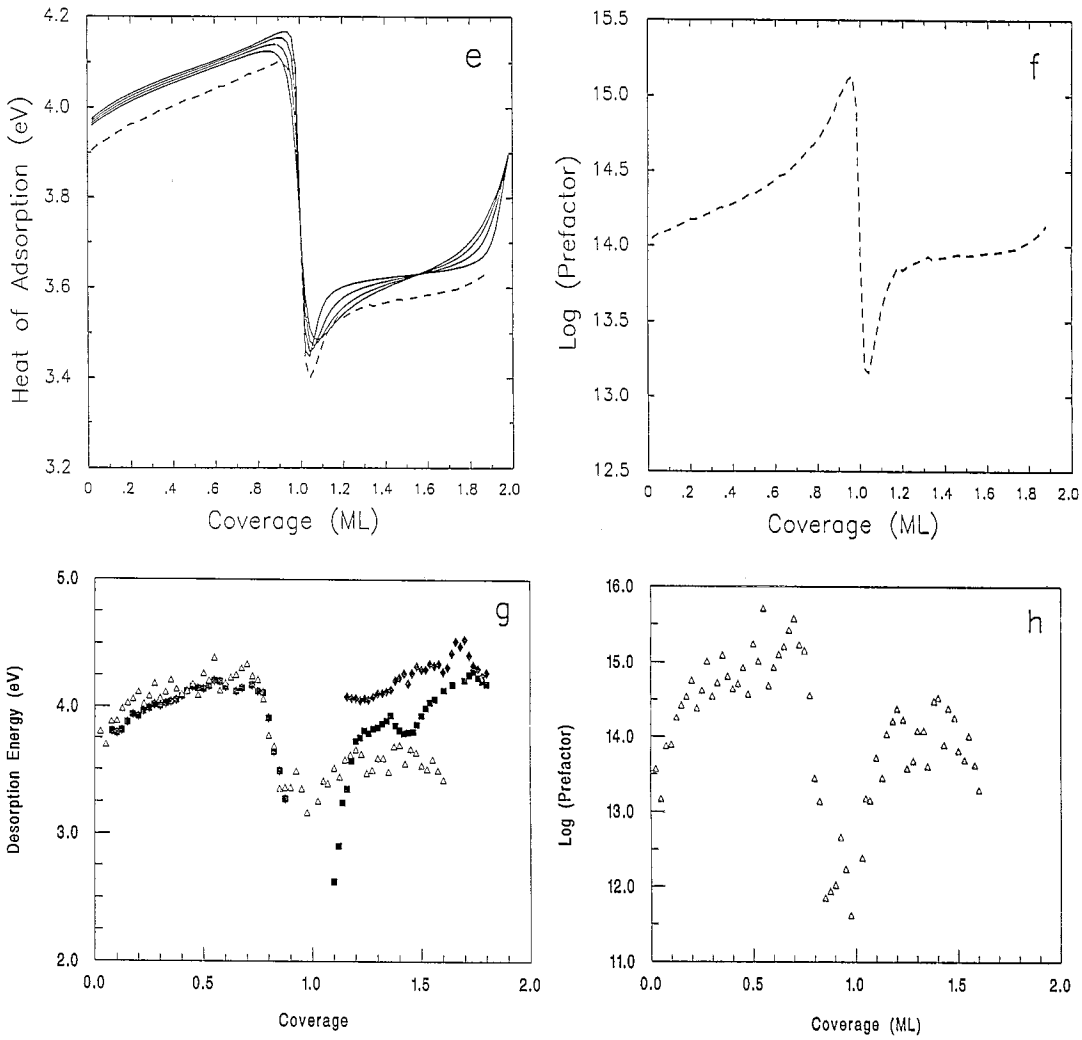

Fig. 2. (a) TPD data of the first two monolayers of Au on Mo(110) obtained with a heating rate of 5.2 K s^{-1}. The curves differ in initial coverage by approximately 0.14 monolayers between 0.07 and 2 monolayers. (b) Theoretical fit for coverages as in Fig. 1b with the following parameters: $V_0^{(1)} = 4.011$ eV, $V_0^{(2)} = 3.38$ eV, $V_{11} = -0.06$ eV, $V_{12} = 0$ eV, $V_{22} = -0.164$ eV, $\nu_x = \nu_y = \nu_z = 3.6 \times 10^{12}$ s^{-1}. (c) Partial coverages for first (———) and second (- - -) layers as a function of temperature. (d) Partial rates for first (———) and second (- - -) layers as a function of temperature. (e) Isosteric heat of adsorption for $T = 1100$, 1200, 1300, 1400 K (top to bottom). Dashed line is the desorption energy obtained from an isosteric Arrhenius analysis of the theoretical curves. (f) Effective prefactor from the Arrhenius analysis of the theoretical curves. (g), (h) The corresponding experimental data.

longer ranged interactions will be discussed after we have looked at the Au/Mo(110) system. In closing we note that our model also gives superb agreement with submonolayer isothermal desorption rate data.

For our second system, Au on Mo(110), the experimental data [4] and a theoretical fit are given in Figs. 2a and 2b. Note that in this system the second layer is bound to the layer below relatively weaker as compared to Cu on Mo(110) and that the nearest neighbor interaction in the first layer is now much less than that in the second layer. As a result, desorption from the first layer at temperatures above 1200 K is from the one-phase region, whereas desorption from the second layer shows the leading edge of zero-order desorption from a two-phase region of the phase diagram. The desorption from the second layer is complicated by a change in the electronic structure and thus in the bonding around 1.4 monolayers [4], a feature that is beyond the present lattice gas model. Our value of $T_c = 1080$ K is close to the experimental value of 1145 K. The growth modes and partial desorption rate in Figs. 2c and 2d indicate layer-by-layer growth for this system as well, even though the substantial overlap of the two peaks would suggest otherwise.

In Figs. 2e and 2f we show the desorption energy and prefactor obtained by a one-line fit to the theoretical isosteric desorption rates [7] (a two-line fit produces differences just above one monolayer, which are minor on the scale displayed). For multi-

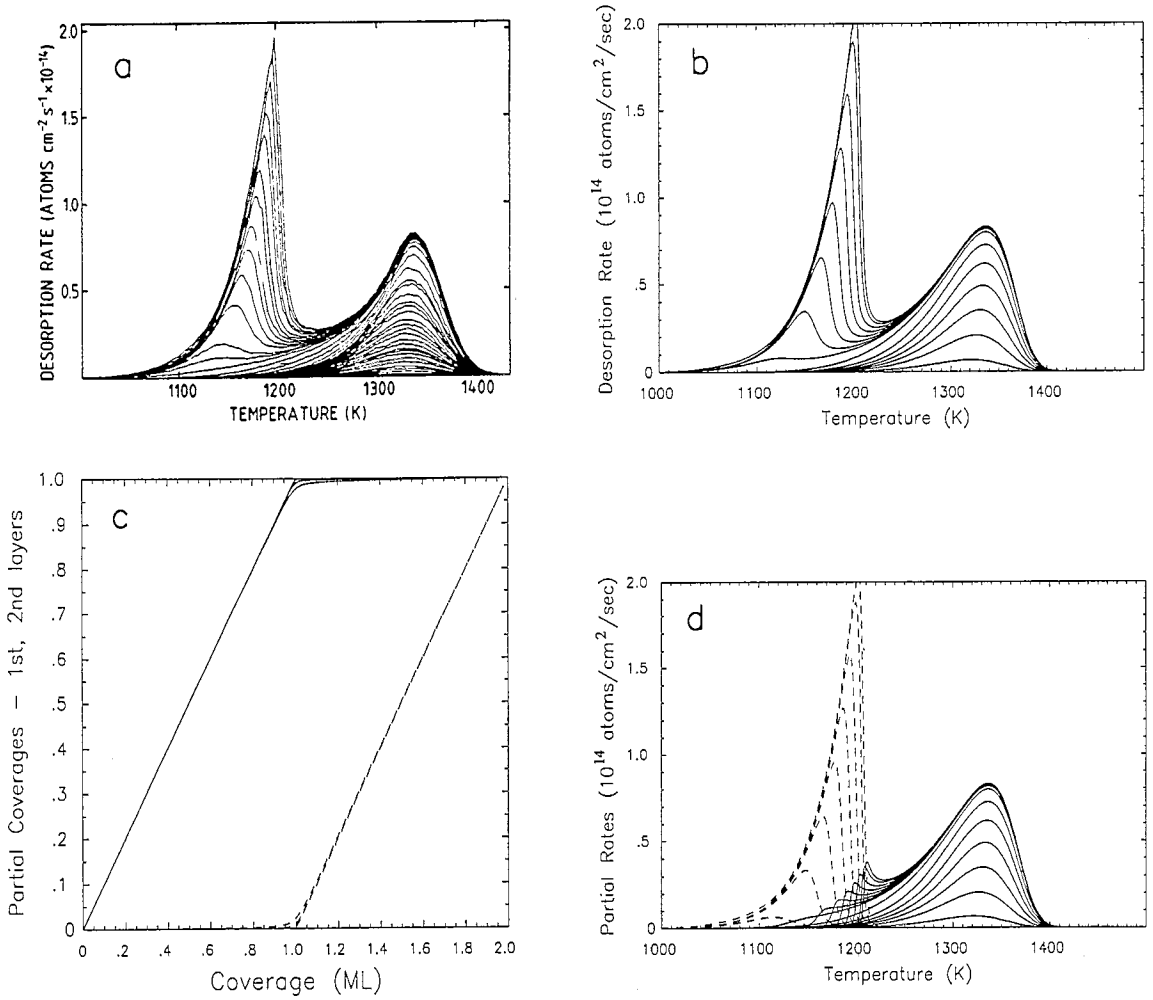

Fig. 2 (continued).

peak TPD data it is sometimes argued that an isosteric analysis should be preceded by a procedure to separate the peaks, e.g. in Figs. 2a and 2b to subtract the first layer peak so that the second layer peak stands alone. The argument for this has been that two peaks in TPD are indicative of two distinct desorption energies, for example, as a result of different adsorption sites. Isosteric rates should thus be a superposition of two Boltzmann factors, which cannot be fitted to a single straight line on an Arrhenius plot. However, one must realize that more frequently two peaks are the result of strong lateral repulsion, e.g. in the submonolayer adsorbate. There is a more compelling reason not to separate a two-peak structure. For an adsorbate maintained in quasi-equilibrium throughout desorption the desorption energy is nothing but a temperature average of the heat of adsorption [6], which is obtained according to Eq. (6) thermodynamically without special tricks associated with peak separation. Indeed, the isosteric analysis of theoretical TPD traces works perfectly well without separating peaks. In desorption from multilayer adsorbates there is yet another reason not to separate peaks associated with the desorption from different layers. Looking at the partial rates in Fig. 2d (and also in Fig. 1d) we note that for desorption from initial coverages larger than one monolayer desorption from the first layer is delayed until the second layer is desorbed completely. At that (higher) temperature desorption from the first layer then sets in abruptly with a spike in the initial rate. Moreover, because the total area under the desorption curve must still account for a complete layer, desorption is generally shifted to higher temperatures. This all implies that for initial coverages larger than one monolayer, desorption of the first monolayer is different from the situation where we started from just one monolayer, and subtraction of the monolayer desorption trace from the spectra for higher initial coverages introduces error. If, on the other hand, the desorption peaks for the first and second layers are well separated (in strict layer-by-layer growth) a layer-by-layer analysis is appropriate because we can then also define thermodynamically the isolated layers for which we, for example, can then define individual critical temperatures, etc.

The original isosteric Arrhenius analysis of the experimental TPD data [4] was done layer-by-layer and is reproduced in Figs. 2g and 2h. There are two major differences to the theoretical model, namely (i) the first layer desorption energy peaks below $\theta \approx 0.8$, whereas the theoretical curve peaks just below the complete monolayer, and (ii) the second layer desorption energy starts at a much lower value than the theoretical model. The first effect is a reflection of the bunching of the TPD traces below a monolayer which does not occur in the theoretical model. Its origin has been speculated to be due to increasing population of the second monolayer during completion of the first. If we, for example, add repulsive trio interactions in the first monolayer, we indeed can produce a drop in the heat of adsorption around $\theta_1 = 0.6$ and a population of the second layer for $\theta < 1$. However, this also fills in the valley between the two desorption peaks and alter the peak rates (lowering and raising the low and high temperature peaks, respectively). Thus, if two peaks in TPD are sufficiently separated (and this is the case for Au) then the system essentially grows in the layer-by-layer mode, and the drop in the desorption energy above $\theta \approx 0.8$ is most likely not due to mass transfer to the second layer. It might reflect a rearrangement of the electronic structure in the adsorbate (as seen in ultrathin Au films on W(110) [9]), which has yet to be explored.

To check the validity of the layer-by-layer analysis, we have re-analyzed the experimental data over both layers doing a one-line fit to the isosteres. The results are also displayed in Figs. 2g and 2h. We essentially reproduce the results of the layer-by-layer analysis except, as expected, in the region just above a monolayer where the complete analysis does not produce as low a dip in the desorption energy. Indeed, desorption energies below 3 eV are accompanied in this system by prefactors of unacceptably low values below 10^{10} s^{-1}.

In our fit to TPD there is another puzzling discrepancy. The critical temperature, T_c, of the first layer resulting from the theory is 400 K. Experimentally, a T_c about twice as high is expected by comparison with Au on W(110) where $T_c = 840$ K was determined by low energy electron diffractometry (LEED) [10]. On the other hand, low energy electron microscopy (LEEM) suggests that crystallization from the two-dimensional vapor in the Au submonolayer on Mo(110) occurs below 600 K [11]. This was

however, a very rough temperature estimate so that the experimental T_c for Au on Mo(110) in the submonolayer range is an open question that must be settled by future LEED or LEEM experiments. If we increase V_{11} to reproduce the higher critical temperature, a reasonable fit to the TPD data can no longer be obtained.

In this Letter we have analyzed two systems, Cu/Mo(110) and Au/Mo(110), for which a multilayer lattice gas gives excellent fits to TPD data, both in shape and in absolute magnitude of the rates. The theory is essentially exact employing transfer matrix methods. The quality of the theoretical fits is nevertheless surprising as the model so far assumes nearest neighbor interactions only, a centered rectangular lattice and on-top adsorption for the second layer, whereas on a bcc (110) the second layer atoms are fourfold coordinated to the first layer. We suspect that taking proper account of the coordination will change the numerical value of the second layer binding energy, $V_0^{(2)}$, but will not change the qualitative feature of layer-by-layer growth as a three-fold coordinated atom in the second layer prevents three first layer atoms from desorbing whereas an on-top atom only inhibits the desorption of one. Indeed, we have tested this in a one-dimensional system by comparing on-top and bridge bonded configurations, which give essentially identical TPD spectra except for system with repulsive interactions in the first layer. This will be discussed elsewhere.

Why can we fit the data with a model with nearest neighbor interactions only, when it is known that longer ranged interactions are operative in metal overlayers? For both systems desorption occurs below or slightly above the critical temperature where strong clustering of the adsorbate is observed. As long as the two-dimensional adsorbate clusters have maximum density, i.e. few vacancies, they are dominated by nearest neighbor interactions. Indeed, the interaction parameters are not uniquely determined by TPD spectra alone. For example, in the first monolayer we can reduce the nearest neighbor attraction by 50% and include a second neighbor attraction of that amount and still obtain TPD spectra that are essentially the same. To pin down the interaction parameters more precisely one needs more information, for example, the detailed shape of the phase diagram at lower temperatures. Using Redhead's formula somewhat liberally one could say that interaction energies that are smaller than $30\Delta T$ have no observable effect on TPD data, where ΔT is the temperature accuracy of the data, which is typically a few tenths of a percent of the mean desorption temperature. (The numerical factor 30 is appropriate for a heating rate of 5 K s^{-1} and a prefactor of 10^{13} s^{-1}.)

Next we want to address the question how our interaction parameters for Cu and Au on Mo(110) compare to those established for these adsorbates on W(110)? Although the W(110) and Mo(110) surfaces are very similar there are profound quantitative and even qualitative differences. Bauer [1] and Roelofs and Bellon [12] have extracted interaction energies for Cu and Au on W(110) from the model calculations of Gollisch [13]. The binding energy of an isolated Au atom on W(110) is about 0.25 eV higher than that of a Cu atom, whereas on a Mo(110) surface we find a difference of about 0.5 eV with the absolute values the same within 10%. Nearest neighbor interactions in the first layer for Cu on W(110) and Mo(110) are similar, -0.223 and -0.172 eV, respectively, but vastly different for Au, namely -0.293 and -0.06 eV, respectively. The latter difference is of course reflected in the different critical temperatures. There is also strong evidence both experimentally [14] and theoretically [13] that on the W(110) surface noble metals form stable dimers and trimers leading, for example, to pronounced plateaus in the desorption energy at low coverages. Whether these plateaus are actually manifestations of a dimer phase is not clear at this stage, but their absence on the Mo(110) surface is worth noting (and puzzling). Before we can hope to resolve such differences we must improve our model by (i) accounting for the proper lattice structure, (ii) by including longer ranged and trio interactions, and (iii) by considering the effect of the shallow adsorption troughs on the structure of the adsorbate. In this context it might also be interesting to study multilayer adsorption and desorption of noble metals on other metal substrates where similar growth modes have been observed.

Acknowledgement

This work was supported in part by a grant from the Office of Naval Research.

References

[1] E. Bauer, Appl. Phys. A 51 (1990) 71.
[2] S.H. Payne and H.J. Kreuzer, Surf. Sci. (1995), submitted.
[3] M. Paunov and E. Bauer, Appl. Phys. A 44 (1987) 201; Surf. Sci. 188 (1987) 123.
[4] A. Pavlovska, H. Steffen and E. Bauer, Surf. Sci. 195 (1988) 207.
[5] H.J. Kreuzer and Z. Jun, Appl. Phys. A 51 (1990) 183.
[6] H.J. Kreuzer and S.H. Payne, in: Dynamics of Gas–Surface Collisions, Eds. M.N.R. Ashfold and C.T. Rettner (Roy. Soc. of Chemistry, Cambridge, 1991).
[7] The analysis of the TPD data was performed with the ASTEK package written by H.J. Kreuzer and S.H. Payne (available from Helix Science Applications, Box 49, Site 3, R.R. 5, Armdale NS, B3L 4J5, Canada).
[8] M. Tikhov and E. Bauer, unpublished.
[9] H. Knoppe and E. Bauer, Phys. Rev. B 48 (1993) 5621.
[10] D. Georgiev and E. Bauer, to be published.
[11] M. Mundschau, E. Bauer, W. Tieleps and W. Świèch, Surf. Sci. 213 (1989) 381.
[12] L.D. Roelofs and R.J. Bellon, Surf. Sci. 223 (1989) 585.
[13] H. Gollisch, Surf. Sci. 175 (1986) 249.
[14] J. Kolaczkiewicz and E. Bauer, Surf. Sci. 160 (1985) 1.